

Sortilin-mediated translocation of ACSL1 impairs non-shivering thermogenesis

Yong Chen (✉ tj.y.chen@vip.163.com)

Tongji Hospital, Tongji Medical College, Huazhong University of Science and Technology
<https://orcid.org/0000-0002-3634-0328>

Min Yang

Tongji Hospital, Tongji Medical College, Huazhong University of Science and Technology

Zengzhe Zhu

Tongji Hospital, Tongji Medical College, Huazhong University of Science and Technology

Rui He

Tongji Hospital, Tongji Medical College, Huazhong University of Science and Technology

Danpei Li

Tongji Hospital, Tongji Medical College, Huazhong University of Science and Technology

Zhihan Wang

Tongji Hospital, Tongji Medical College, Huazhong University of Science and Technology

Yuyu Xie

Tongji Hospital, Tongji Medical College, Huazhong University of Science and Technology

Huanyu Wang

Tongji Hospital, Tongji Medical College, Huazhong University of Science and Technology

Hongyan Deng

Tongji Hospital, Tongji Medical College, Huazhong University of Science and Technology

Jiada Liu

Tongji Hospital, Tongji Medical College, Huazhong University of Science and Technology

Xuefeng Yu

Tongji Hospital, Tongji Medical College, Huazhong University of Science and Technology

Ruping Pan

Tongji Hospital, Tongji Medical College, Huazhong University of Science and Technology

Pema Maretich

Department of Biology, Massachusetts Institute of Technology

Shingo Kajimura

Beth Israel Deaconess Medical Center, Harvard Medical School, and Howard Hughes Medical Institute
<https://orcid.org/0000-0003-0672-5910>

Keywords:

Posted Date: March 15th, 2023

DOI: <https://doi.org/10.21203/rs.3.rs-2667036/v1>

License:   This work is licensed under a Creative Commons Attribution 4.0 International License.

[Read Full License](#)

Abstract

Obesity and its related metabolic disorders are caused by an imbalance between homeostatic energy consumption and expenditure. Brown and beige adipose tissues have been shown to be protective against these diseases due to their critical roles in non-shivering thermogenesis; additionally, adrenergic innervation of these cells promotes lipolysis and fatty acid oxidation¹. A key enzyme promoting fatty acid oxidation in adipose tissues, particularly in response to cold-stimulus, is mitochondrial acyl-CoA synthetase long-chain family member 1 (ACSL1)². However, the regulatory mechanism of the subcellular localization of ACSL1 in adipocytes remains poorly understood. Here, we identify an endosomal trafficking component sortilin (encoded by *Sort1*) in adipose tissues that facilitates the translocation of ACSL1 from mitochondria to lysosome for further degradation. In brown and beige adipose tissues, sortilin is downregulated upon adrenergic stimulation but its levels are restored to baseline after the stimulus is withdrawn. Depletion of *Sort1* in adipocytes results in an increase in whole body energy expenditure. Moreover, mice with adipose-specific *Sort1* depletion are resistant to high-fat diet (HFD)-induced obesity and insulin resistance. Collectively, our findings identify sortilin as a promising therapeutic target that negatively regulates non-shivering thermogenesis in adipocytes by promoting the translocation of ACSL1 from the mitochondria to lysosome.

Highlights

- Cold stimulus and subsequent adrenergic activation decrease sortilin levels in adipocytes; sortilin levels return to baseline after the removal of the stimulus.
- Sortilin regulates non-shivering thermogenesis by tuning the trafficking of ACSL1 between mitochondria and lysosome.
- Adipose-specific *Sort1*-depleted mice are resistant to hypothermia and obesity.
- Therapeutic administration of sortilin inhibitors promotes energy expenditure and improves

Introduction

The ever-growing public health burden of obesity and its related disorders, such as type 2 diabetes and cardiovascular diseases, has led to a considerable amount of resources spent countering this problem³⁻⁵. Nevertheless, effective treatments for obesity remain elusive due to inadequate lifestyle changes or grave side effects from current medical interventions⁶⁻⁸. Thus, novel therapeutics for obesity with minimal side effects are urgently needed. Obesity is caused by an imbalance in energy metabolism, with energy intake chronically exceeding energy expenditure. The result is an ectopic and excessive accumulation of harmful lipids in multiple tissues, predominantly adipose tissue⁵. In healthy individuals, adipose tissue also functions as a dynamic endocrine organ that is critical for maintaining homeostasis. Emerging evidence suggests that adipose tissue dysfunction is a critical component of obesity-associated pathologies^{5,9,10}. Notably, fat depots contain heterogeneous populations of white, brown, and beige adipocyte, that can be classified based on their anatomical locations and metabolic

functions^{1,11,12}. Unlike white adipocytes, brown and beige adipocytes are mitochondria-rich and play a key role in driving non-shivering thermogenesis and energy expenditure, thus making them promising targets for combating obesity and its concomitant metabolic disorders^{1,13-15}.

Canonically, brown and beige adipose thermogenesis is induced by catecholamines (noradrenaline, NA) through the β 3-adrenergic receptor¹⁶. β 3-adrenergic signaling activates intracellular cAMP signaling to then induce lipolysis and oxidative phosphorylation in brown/beige adipocytes. These adipocytes dissipate heat instead of generating ATP via both uncoupling protein 1 (UCP1)-dependent and UCP1-independent pathways^{1,17-20}. Brown and beige fat activation has been shown to be a promising approach to combat obesity^{1,17-20}. However, due to a myriad of off-target effect, as well as the cardiovascular stress inherent in stimulating β 3 adrenergic signaling, effective therapeutics targeting this receptor remain largely unrealized^{21,22}. Downstream of β 3 adrenergic signaling stimulates lipolysis and fatty acid β -oxidation (FAO). Promoting lipolysis and FAO activate brown and beige adipocytes, which can be used as a more promising therapeutic target for obesity^{23,24}.

Specifically, fatty acids released from NA-induced lipolysis serve as both obligatory activators for UCP1 and metabolic substrates fueling thermogenic respiration²⁵⁻²⁷. Following lipolysis from triglycerides (TGs), fatty acids are converted to ACSL1 and specifically directed toward mitochondrial FAO. ACSL1 is enriched in mitochondria and the mitochondria FAO is crucial for much of the metabolic benefits derived from brown adipose tissue (BAT) activity as well as BAT maintenance²⁸. ACSL1 is reported to localize both in mitochondria and in endoplasmic reticulum (ER) in adipocytes²⁹. When localized to the outer mitochondrial membrane, ACSL1 generates long-chain acyl-CoA destined for β -oxidation; acyl-CoA is converted to acylcarnitine in the mitochondrial matrix for tricarboxylic acid cycle (TCA)³⁰. However, the regulatory mechanism of the subcellular localization of ACSL1 in adipocytes remains unknown. Here, we identified sortilin, an endosomal trafficking component, regulates the trafficking of ACSL1 between mitochondria and lysosome. The endosomal system controls signalling involved in metabolic physiology by tuning the trafficking and distribution of key proteins. Some of the core machineries involved in the endosomal system are altered in metabolic diseases. Tuning the endosomal system could improve metabolic parameters in metabolic diseases and is regarded as a potential novel therapeutic strategy for metabolic pathologies³¹. Sortilin, which is one of the targeted endosomal components and involved in trans-Golgi trafficking to late endosomes and the plasma membrane, plays an important role in lipid metabolism³²⁻³⁴. For example, sortilin has an essential role in the secretion of ApoB-containing VLDLs. Besides, sortilin colocalizes with PCSK9 in the trans-Golgi network and facilitates its secretion from primary hepatocytes³⁵. In addition, sortilin is also known as neurotensin receptor 3 (NTSR3). Neurotensin (NTS) secreted from lymphatic vessels in brown adipose tissue plays an inhibitory role in adaptive thermogenesis³⁶. NTS has three receptors (NTSR1, NTSR2 and sortilin). NTSR1 is not expressed on adipocytes. NTSR2 is the receptor that mediates the thermogenic inhibition of neurotensin³⁶. Unlike NTSR1/2, which are G-protein coupled receptors and specific receptors for neurotensin, sortilin is a type I transmembrane protein that belongs to the family of Vps10p-domain receptors³⁷⁻⁴². The role of sortilin

in adipocytes thermogenesis is not yet known. Adipose tissue undergoes thermogenic remodeling in response to thermal stress. In this study, we found that cold stimulus and subsequent adrenergic activation decrease sortilin levels in adipocytes; sortilin levels return to baseline after the removal of the stimulus. This indicates adrenergic activation modifies the components of endosomal system in thermogenic adipocytes. Adipocyte-specific depletion of *Sort1* induced significant increases in metabolic activity and non-shivering thermogenesis. We used mass spectrometry-based proteomics to identify ACSL1-sortilin protein interactions. Sortilin facilitated the translocation of mitochondrial ACSL1 to lysosomes for further degradation. Relative to controls, the mitochondria of *Sort1*-depleted beige adipocytes were enriched for ACSL1 and late lysosomal enrichment was reduced. This illustrates that adipose tissue undergoes thermogenic remodeling in response to thermal stress and adrenergic activation regulates non-shivering thermogenesis by tuning the expression of sortilin in adipocytes. We also found that mice with adipose-specific *Sort1* deletion were resistant to high-fat diet (HFD)-induced obesity and insulin resistance. These findings reveal that sortilin represents a novel therapeutic target for treating obesity.

Results

Sortilin expression is inhibited by cold stimulus and positively correlated with obesity

We found that sortilin expression was significantly reduced in BAT and inguinal adipose tissue (iWAT) following three days of cold exposure and seven days of treatment with the β 3-AR agonist CL316,243 (Fig. 1b-e and Extended Data Fig. 1a, b). After the stimulus was removed, the expression of sortilin was restored in iWAT and partially restored in BAT. Interestingly, sortilin expression was inversely correlated to that of UCP1 (Fig. 1b-e). To elucidate the relationship between sortilin and obesity, we quantified the mRNA expression of *Sort1* in omental adipose tissue of obese patients along with their circulating metabolite profile. *Sort1* mRNA levels were significantly upregulated in obese patients (Fig. 1f) and were positively correlated with waist circumference and BMI (Fig. 1g, h). Moreover, upregulated *Sort1* expression was significantly correlated with low-density lipoprotein C (LDL-C) (Fig. 1i) but not with TG, high-density lipoprotein C (HDL-C), blood glucose, ALT and creatinine (Fig. 1j and Extended Data Fig. 1d-f). In summary, sortilin was reduced by cold challenge but elevated after acclimating back to room temperature. The enrichment of sortilin in white fat was positively associated with obesity and its established metabolic features.

Sort1 depletion enhances fat thermogenesis

We next compared the transcriptional profiles between epididymal white adipose tissue (eWAT) and BAT of several public microarray datasets from the Gene Expression Omnibus (GEO) database. We found that the mRNA expression of *Sort1* was significantly lower in mouse BAT than in eWAT (Extended Data Fig. 2a). We further verified the mRNA expression of *Sort1* in eWAT, iWAT, BAT and muscle in wild-type mice and found that the expression of *Sort1* was enriched in adipose tissues and the expression was highest in eWAT, lower in iWAT, and lowest in BAT (Fig. 2a, b). We also compared the expression of *Sort1*

in mature adipocytes extracted from the above three adipose tissues, and observed similar, though more striking, trends (Extended Data Fig. 2b). Besides, the expression of *Sort1* was lower in primary brown and beige adipocytes after forskolin treatment (Extended Data Fig. 2c, d). Accordingly, we asked whether sortilin depletion would affect fat thermogenesis. To answer this question, we cultured immortalized adipocytes that were differentiated from BAT and iWAT isolated stromal-vascular fractions (SVFs). The expression of sortilin was highly upregulated in differentiated mature brown and beige adipocytes but was hardly expressed in SVF (Fig. 2c, d). We constructed a lentivirus to deplete *Sort1* (shSort1) in SVFs. Depletion of *Sort1* did not inhibit beige adipocytes differentiation (Fig. 2e) but significantly enhanced both the basal and maximal oxygen-consumption rates (OCRs) (Fig. 2f). Depletion of *Sort1* also increased basal OCR in human beige adipocytes (Extended Data Fig. 2f) and free glycerol release in mouse brown adipocytes (Extended Data Fig. 2e). In addition, we conducted RNA-seq analysis in *Sort1*-depletion beige adipocytes to better understand the mechanism by which *Sort1* exerted its effects. Gene set enrichment analysis (GSEA) revealed that *Sort1* depletion activated the expression of genes enriched in thermogenesis, fatty acid metabolism and oxidative phosphorylation pathways (Fig. 2g-i). The above data indicate that sortilin accumulates in white adipocytes and *Sort1* depletion activates the thermogenesis of brown and beige fat.

Sortilin interacts with ACSL1 and controls its protein degradation

To explore the underlying mechanism of thermogenesis triggered by *Sort1* depletion in adipocytes, we used mass spectrometry-based proteomics to identify proteins that interact with sortilin. Sortilin accumulated in mouse white fat and adult human BAT depots from the supraclavicular and other regions contain UCP1-positive adipocytes that exhibit molecular signatures resembling murine beige adipocytes^{43,44}, so we focused on mouse beige adipocytes to explore the specific mechanism. First, we extracted proteins from fully differentiated beige adipocytes for further immunoprecipitation (IP) by sortilin and vehicle IgG antibody for protein capture. The precipitated proteins were then subjected to mass spectrometry analysis (Fig. 3a). A total of 394 proteins were coprecipitated with sortilin, of which only the ACSL1 protein was enriched in the above three activated pathways (thermogenesis, fatty acid metabolism and oxidative phosphorylation) (Fig. 3b and Extended Data Fig. 3a). To verify the findings from the proteomics analysis, we used both sortilin-and ACSL1-specific antibodies to pull down interacting proteins and then confirmed their presence using western blot. Sortilin antibodies were able to pull down ACSL1 proteins and vice versa (Fig. 3c, d). The physical interaction between sortilin and ACSL1 was further confirmed in beige adipocytes via immunofluorescence assays (Fig. 3e). We further probed the functional interactions between sortilin and ACSL1 and found that *Sort1* depletion markedly enhanced the protein expression of ACSL1 (Fig. 3f). Furthermore, cycloheximide chase assays showed that *Sort1* depletion significantly extended the half-life of the ACSL1 protein (Fig. 3g). SVF cells were transfected with shRNA targeting *Acs/1*. *Acs/1* mRNA levels were reduced by nearly 50% in fully differentiated adipocytes (Extended Data Fig. 3b). To assess the functional consequence of *Acs/1* depletion, we measured the cell OCR and the amount of media glycerol, two important markers for thermogenesis capacity. Depletion of *Acs/1* resulted in significantly decreased levels of glycerol accumulated in the media following vehicle or forskolin stimulation, consistent with decreased basal

lipolysis (Extended Data Fig. 3c). Correspondingly, the ACSL1 inhibitor triacsin C resulted in greatly decreased glycerol levels following forskolin stimulation and basal OCR levels (Extended Data Fig. 3d, e). These results support a physical and functional interaction between sortilin and ACSL1 and suggest that this interaction may regulate adipocyte thermogenesis.

Sortilin targets mitochondrial ACSL1 for lysosomal degradation to regulate thermogenesis

To further evaluate the specific mechanism of the increased protein expression of ACSL1 mediated by sortilin, we extracted mitochondria from shcon and shSort1 beige adipocytes. The results showed increased enrichment of ACSL1 in both the mitochondria and cytosol but mainly in the mitochondria (Fig. 4b). Accordingly, we found that ACSL1 was predominantly enriched on mitochondria by confocal microscopy in *Sort1*-depletion adipocytes (Fig. 4a). We next employed inhibitors of various protein degradation pathways to determine how ACSL1 is degraded. Interestingly, inhibition of lysosomes by either NH₄Cl or chloroquine inhibited sortilin-induced downregulation of ACSL1 (Fig. 4c, d). However, inhibition of autophagy (with 3-MA) or the proteasome (with MG132) did not lead to any change in sortilin-induced ACSL1 downregulation (Extended Data Fig. 4a, b). As expected, depletion of *Sort1* significantly decreased the distribution of ACSL1 to lysosomes (LAMP1 and EEA1, Fig. 4e, f). To further probe the effect of ACSL1 degradation on thermogenesis, we transfected adipocytes with small interfering (si) RNA against ACSL1 and then performed glycerol and OCR assays. Treatment of cells with ACSL1 siRNA reduced the expression of ACSL1 (Fig. 4g). The activation effects of *Sort1* deletion on OCR and glycerol were eliminated in cells transfected with ACSL1 siRNA (Fig. 4h, i), demonstrating that *Sort1*-mediated regulation of adipocyte thermogenesis operates through the regulation of ACSL1. We also incubated beige adipocytes with the ACSL1 inhibitor (triacsin C). Similarly, the inhibitor significantly diminished the *Sort1* depletion-induced increase in OCR (Extended Data Fig. 4d, e). These findings suggest that sortilin may regulate thermogenesis by inhibiting the levels of mitochondrial ACSL1 in a lysosome-dependent manner.

Sort1 depletion restrains the development of HFD-induced obesity

To investigate whether the increase in thermogenesis mediated by *Sort1* depletion improves systemic metabolism, we established two animal models of *Sort1* depletion to study the effects of this depletion on whole body metabolism. First, we generated adipocyte conditional *Sort1*-deletion (*Sort1*^{AKO}) mice using the clustered regularly interspaced short palindromic repeats (CRISPR)/CRISPR-associated protein 9 (Cas9) system (Fig. 5a). The deletion of *Sort1* in adipose tissue but not in the liver was confirmed by qPCR and immunoblot (Fig. 5b, c). We subjected *Sort1*^{AKO} mice and littermates to a HFD challenge. *Sort1*^{AKO} mice gained significantly less body weight than *Sort1*^{fl/fl} mice (Fig. 5d, e). Consistently, the weights of adipose tissues, including BAT, iWAT and eWAT, as well as liver tissue, were markedly decreased in *Sort1*^{AKO} mice compared to *Sort1*^{fl/fl} mice (Fig. 5f). The diameters of adipocytes in BAT, iWAT, and eWAT were significantly smaller in *Sort1*^{AKO} mice than in *Sort1*^{fl/fl} mice (Fig. 5g). All results above account for that *Sort1*^{AKO} mice promoted significant metabolic improvements. Furthermore, the glucose tolerance test (GTT) and insulin tolerance test (ITT) revealed that *Sort1*^{AKO} mice exhibited a more

efficient clearance of plasma glucose than *Sort1^{fl/fl}* mice after HFD feeding, as evidenced by reduced areas under the curve (AUC) of GTT and ITT, respectively (Fig. 5h, i). In addition, unlike those of HDL-C and free fatty acids (FFAs), the concentrations of plasma TGs, cholesterol and LDL-C were all significantly lower in *Sort1^{AKO}* mice than in *Sort1^{fl/fl}* mice (Fig. 5j). Lipid accumulation and TG content in the liver were also lower in *Sort1^{AKO}* mice than in *Sort1^{fl/fl}* mice (Fig. 5k-l).

We also performed a loss-of-function study *in vivo* using an adeno-associated virus (AAV) that expresses short hairpin RNAs directly targeting *Sort1* (shSort1). Direct injection of AAVshSort1 into the iWAT of wild-type mice resulted in a 60% lower mRNA expression of *Sort1* in iWAT compared to that in the mice that received an AAV with a scrambled control shRNA (AAVshcon) (Extended Data Fig. 5a-c). These mice were then subjected to HFD challenge, which revealed that AAVshSort1 mice featured decreased adiposity compared with AAVshcon mice, as shown by decreased body weights, adipose tissue weights, and adipocyte sizes as well as improved insulin resistance and hepatic steatosis (Extended Data Fig. 5d-l). However, when the mice were fed a normal diet (ND), there was not much difference between AAVshSort1 mice and AAVshcon mice in their body weight and glucose tolerance. Together, these data suggest that *Sort1* depletion can prevent obesity and metabolic comorbidities.

Sort1 depletion promotes thermogenesis and energy expenditure *in vivo*

We next examined whether *Sort1* depletion affects whole body energy balance. *Sort1^{AKO}* mice with a persistent HFD showed significantly higher oxygen consumption and energy expenditure than *Sort1^{fl/fl}* mice with unaltered food intake (Fig. 6a-c). *Sort1^{AKO}* mice displayed a higher core temperature during cold exposure and were more resistant to cold-induced hypothermia than *Sort1^{fl/fl}* mice (Fig. 6d-f). These results demonstrate that under stressful conditions such as cold exposure or HFD feeding, *Sort1* deletion markedly increased thermogenesis and energy expenditure. To verify this, mice with specific depletion of *Sort1* in iWAT (AAVshSort1) displayed a higher systemic energy expenditure than the control mice even under thermal neutrality (Extended Data Fig. 6b, c). These results suggest that *Sort1* depletion promotes thermogenesis and energy expenditure *in vivo*.

Sortilin inhibitor AF38469 promotes fat thermogenesis with promising therapeutic potential

In light of the current global obesity epidemic, promising targets and approaches to achieve safe and effective activation of brown/beige fat are urgently needed. AF38469 is an orally bioavailable inhibitor of sortilin⁴⁵. We first investigated the effects of AF38469 on beige adipocytes. As expected, AF38469 treatment in these cells led to an upregulation of ACSL1 expression (Fig. 7b). Moreover, AF38469 treatment in adipocytes caused an elevation in cellular respiration, as verified by an increased OCR and proton leak (Fig. 7c). To further evaluate the effect of AF38469 treatment *in vivo*, particularly with respect to energy consumption and metabolism, we administered AF38469 to wild-type mice orally in the drinking water. Strikingly, AF38469-treated mice after HFD challenge showed significantly lower body weights; BAT, iWAT, and eWAT masses (Fig. 7e-g). In addition, AF38469-treated mice showed greater glucose tolerance and insulin sensitivity than the control mice (Fig. 7h, i). Notably, AF38469-treated mice displayed a substantially elevated energy expenditure compared to those of the control mice, without

differences in food intake (Fig. 7j-l). No significant changes in body weight were observed when the mice were fed a chow diet, but the glucose tolerance of the mice was improved (Extended Data Fig. S7b, c). Importantly, AF38469 treatment did not result in any hepatotoxicity, as the plasma levels of enzymes (ALT and AST) were not altered after AF38469 administration (Extended Data Fig. 7d). In summary, sortilin inhibition using commercially available drugs promotes energy expenditure and has been shown to reverse critical metrics to metabolic dysregulation associated with obesity.

Discussion

Thermogenesis in brown and beige adipocytes protects animals from hypothermia and obesity. The signaling cascades that promote adipose tissue thermogenesis have been extensively described, yet little is known about the inhibition of these pathways. Here, we show that sortilin acts as an inhibitor of adipose thermogenesis. The expression of sortilin is decreased upon cold exposure and increased after withdrawal of the cold stimulus. Sortilin directly targets ACSL1, the rate-limiting enzyme in mitochondrial FAO, leading to ACSL1 degradation by the lysosome. Thermogenic adipocytes have particularly large numbers of mitochondria; by restricting mitochondrial oxidative phosphorylation, sortilin prevents unexpected mitochondrial damage and cell death⁴⁶. While non-shivering thermogenesis can be beneficial in pathological states such as obesity, it also can be a waste of caloric energy in normal healthy individuals. Sortilin potentially serves to fine tune energy homeostasis, which may confer a survival advantage to animals when food is scarce. Interestingly, in the case of abundant food supply and excessive energy intake, removing this restriction will increase heat production, thus greatly helping to cure diseases caused by excess energy, i.e., obesity and type 2 diabetes.

The severity of the obesity epidemic warrants further aggressive intervention. Currently, six major FDA-approved drugs have been used as anti-obesity medications. These drugs can be classified into two types: anorectics to suppress appetite and pancreatic lipase inhibitors to reduce intestinal fat absorption. Unfortunately, most of them have undesirable adverse effects⁴⁷. Previous studies have implemented cold stimuli or adrenergic signaling activation as a useful way to activate brown and beige fat for obesity treatment^{27,48}. However, these treatments have limited applications because of various health concerns and potential cardiovascular hazards^{21,49,50}. Thus, given the obesity epidemic, promising approaches to achieve safe and effective brown and beige fat activation are urgently needed. In the present study, we demonstrated that sortilin plays a critical role in HFD-induced obesity and systemic insulin resistance. We demonstrated that genetic depletion of sortilin or administration of the sortilin inhibitor AF38469 to dietary mouse models of obesity reduced weight and enhanced insulin resistance. Of clinical significance, we revealed the association of decreased *Sort1* abundance in visceral adipose tissues with lower human BMI and improved metabolic traits. This study offers evidence of the positive effect of AF38469 in treating obesity and metabolic diseases and suggests that it would be worthwhile to utilize AF38469 as a therapeutic target for the treatment of obesity. Consistently, we found no severe adverse effects in mice orally treated with AF38469 upon long-term observation. Further studies are needed to optimize the molecular mechanism and evaluate the safety of AF38469.

Lipolysis is essential for adipose tissue thermogenesis, as the fatty acids released from NA-induced lipolysis serve as metabolic substrates fueling thermogenic respiration. The activation of fatty acids is regulated by a set of enzymes called acyl-CoA synthetase long-chain isoforms (ACSLs). As previously reported, the expression levels of ACSL family members in thermogenic tissues determined the substrate availability for β -oxidation and consequently the thermogenic capacity; ACSLs have been reported to be abundant in adipose, liver, and heart tissues⁵¹. ACSL1 contributes to 80% of the total ACSL activity in adipose tissue. When localized to the outer mitochondrial membrane, ACSL1 generates long-chain acyl-CoA for β -oxidation in mitochondria, and fatty acid oxidation is reduced in adipocyte-specific *Acs1* KO mice^{2,52,53}. In the present study, sortilin was identified as a new regulator of ACSL1. *Sort1*-depleted adipocytes had greater ACSL1 expression than control beige adipocytes. Most of the ACSL1 was distributed on mitochondria, and due to the increased expression, the ACSL1 could channel more acyl-CoA to mitochondria for oxidation. Previous studies showed sortilin is involved in trans-Golgi trafficking to late endosomes^{35,54}. In this study, sortilin degrades ACSL1 exclusively in a lysosomal-dependent manner, not by autophagy and ubiquitination. This was consistent with previous studies and laterally highlighted the pivotal role of sortilin as an endosomal component target for metabolic homeostasis and diseases³¹.

Glucose transporter 4 (GLUT4) is expressed in adipocytes and muscle cells, where it regulates the uptake of glucose in an insulin-responsive manner. Previous studies showed that sortilin mediated the intracellular transport of GLUT4 in 3T3-L1 adipocytes^{55,56}. In this study, GLUT4 was also one of the extracted proteins that was immunoprecipitated by sortilin in beige adipocytes. Glucose uptake in thermogenic fat was stimulated in two metabolic states: sympathetically stimulated during active thermogenesis or stimulated by insulin during active anabolic processes. Insulin-stimulated glucose uptake in thermogenic fat is well characterized to occur via the PI3K/Akt pathway, resulting in the rapid translocation of GLUT4 from intracellular vesicles to the cell membrane³¹. In contrast, cold or β 3-adrenoceptor activation increases glucose uptake through rapid de novo synthesis of GLUT1 by cAMP and subsequent translocation of GLUT1 to the plasma membrane⁵⁷. In addition, the GLUT4 inhibitor indinavir does not inhibit isoproterenol-stimulated glucose uptake while inhibiting insulin-mediated glucose uptake^{57,58}. This finding highlights a contrast between the mechanisms of insulin and β 3-adrenoceptor-mediated glucose uptake in thermogenic fat^{59,60}. Consistently, we found depletion of sortilin increased glucose uptake in beige adipocytes and adipocyte-specific *Sort1* depleted mice had improved systemic glucose clearance.

Thus, future research elucidating the role of endosomal trafficking in metabolic regulation are warranted; in particular, the dynamic processes regulating activity of the endosomal pathway control the distribution of more than 5,000 integral membrane proteins - many of which are metabolic transporters, signaling receptors and ligands⁶¹. It has been shown using organelle proteomics that the livers of mice fed a HFD undergo a redistribution of their subcellular structures, strongly suggesting changes intracellular transport in disease states such as obesity⁶². Furthermore, RNA sequencing datasets from rats fed a HFD revealed that genes encoding components of the endosomal membrane were differentially enriched⁶³. By

targeting the endosomal sorting receptor, sortilin, our work highlights this receptor as a critical negative regulator of mitochondrial β -oxidation, and offers preliminary evidence that modulating endosomal pathways may be a viable approach to treating obesity-related metabolic disorders.

Declarations

DECLARATION OF INTERESTS

All authors declare that they have no competing interests.

References

1. Cohen, P. & Kajimura, S. The cellular and functional complexity of thermogenic fat. *Nat Rev Mol Cell Biol* **22**, 393-409, doi:10.1038/s41580-021-00350-0 (2021).
2. Ellis, J. M. *et al.* Adipose acyl-CoA synthetase-1 directs fatty acids toward β -oxidation and is required for cold thermogenesis. **12**, 53-64 (2010).
3. Abarca-Gómez, L. *et al.* Worldwide trends in body-mass index, underweight, overweight, and obesity from 1975 to 2016: a pooled analysis of 2416 population-based measurement studies in 128·9 million children, adolescents, and adults. **390**, 2627-2642 (2017).
4. Wang, Y., Zhao, L., Gao, L., Pan, A. & Xue, H. Health policy and public health implications of obesity in China. *Lancet Diabetes Endocrinol* **9**, 446-461, doi:10.1016/S2213-8587(21)00118-2 (2021).
5. Pan, J., Yin, J., Gan, L. & Xue, J. Two-sided roles of adipose tissue: Rethinking the obesity paradox in various human diseases from a new perspective. *Obes Rev* **24**, e13521, doi:10.1111/obr.13521 (2023).
6. Winslow, D. H., Bowden, C. H., DiDonato, K. P. & McCullough, P. A. J. S. A randomized, double-blind, placebo-controlled study of an oral, extended-release formulation of phentermine/topiramate for the treatment of obstructive sleep apnea in obese adults. **35**, 1529-1539 (2012).
7. Bessesen, D. H. & Van Gaal, L. F. Progress and challenges in anti-obesity pharmacotherapy. *The Lancet Diabetes & Endocrinology* **6**, 237-248, doi:10.1016/s2213-8587(17)30236-x (2018).
8. Kris-Etherton, P. M. *et al.* The Dynamic Interplay of Healthy Lifestyle Behaviors for Cardiovascular Health. *Curr Atheroscler Rep* **24**, 969-980, doi:10.1007/s11883-022-01068-w (2022).
9. Greenberg, A. S. & Obin, M. S. Obesity and the role of adipose tissue in inflammation and metabolism. *Am J Clin Nutr* **83**, 461S-465S, doi:10.1093/ajcn/83.2.461S (2006).
10. Tseng, Y. H. Adipose tissue in communication: within and without. *Nat Rev Endocrinol* **19**, 70-71, doi:10.1038/s41574-022-00789-x (2023).
11. Rosen, E. D. & Spiegelman, B. M. J. C. What we talk about when we talk about fat. **156**, 20-44 (2014).
12. Scheja, L. & Heeren, J. J. N. r. e. The endocrine function of adipose tissues in health and cardiometabolic disease. **15**, 507-524 (2019).

13. Betz, M. J. & Enerbäck, S. J. D. Human brown adipose tissue: what we have learned so far. **64**, 2352-2360 (2015).
14. Bartelt, A. & Heeren, J. J. N. R. E. Adipose tissue browning and metabolic health. **10**, 24-36 (2014).
15. Auger, C. & Kajimura, S. Adipose Tissue Remodeling in Pathophysiology. *Annu Rev Pathol* **18**, 71-93, doi:10.1146/annurev-pathol-042220-023633 (2023).
16. Carmen, G.-Y. & Víctor, S.-M. J. C. s. Signalling mechanisms regulating lipolysis. **18**, 401-408 (2006).
17. Chondronikola, M. *et al.* Brown adipose tissue improves whole-body glucose homeostasis and insulin sensitivity in humans. **63**, 4089-4099 (2014).
18. Lee, P., Werner, C., Kebebew, E. & Celi, F. J. I. j. o. o. Functional thermogenic beige adipogenesis is inducible in human neck fat. **38**, 170-176 (2014).
19. van Marken Lichtenbelt, W. D. *et al.* Cold-activated brown adipose tissue in healthy men. **360**, 1500-1508 (2009).
20. Yoneshiro, T. *et al.* Recruited brown adipose tissue as an antiobesity agent in humans. **123**, 3404-3408 (2013).
21. Larsen, T. M. *et al.* Effect of a 28-d treatment with L-796568, a novel β 3-adrenergic receptor agonist, on energy expenditure and body composition in obese men. **76**, 780-788 (2002).
22. Hainer, V. J. E. O. o. P. Beta3-adrenoreceptor agonist mirabegron—a potential antiobesity drug? **17**, 2125-2127 (2016).
23. Markussen, L. K. *et al.* Lipolysis regulates major transcriptional programs in brown adipocytes. *Nat Commun* **13**, 3956, doi:10.1038/s41467-022-31525-8 (2022).
24. Sveidahl Johansen, O. *et al.* Lipolysis drives expression of the constitutively active receptor GPR3 to induce adipose thermogenesis. *Cell* **184**, 3502-3518 e3533, doi:10.1016/j.cell.2021.04.037 (2021).
25. Blondin, D. P. *et al.* Inhibition of intracellular triglyceride lipolysis suppresses cold-induced brown adipose tissue metabolism and increases shivering in humans. **25**, 438-447 (2017).
26. Fedorenko, A., Lishko, P. V. & Kirichok, Y. J. C. Mechanism of fatty-acid-dependent UCP1 uncoupling in brown fat mitochondria. **151**, 400-413 (2012).
27. Harms, M. & Seale, P. J. N. m. Brown and beige fat: development, function and therapeutic potential. **19**, 1252-1263 (2013).
28. Gonzalez-Hurtado, E., Lee, J., Choi, J. & Wolfgang, M. J. J. M. m. Fatty acid oxidation is required for active and quiescent brown adipose tissue maintenance and thermogenic programming. **7**, 45-56 (2018).
29. Ji, L. *et al.* AKAP1 Deficiency Attenuates Diet-Induced Obesity and Insulin Resistance by Promoting Fatty Acid Oxidation and Thermogenesis in Brown Adipocytes. *Adv Sci (Weinh)* **8**, 2002794, doi:10.1002/advs.202002794 (2021).
30. Huh, J. Y. *et al.* TANK-Binding Kinase 1 Regulates the Localization of Acyl-CoA Synthetase ACSL1 to Control Hepatic Fatty Acid Oxidation. *Cell Metab* **32**, 1012-1027 e1017, doi:10.1016/j.cmet.2020.10.010 (2020).

31. Gilleron, J. & Zeigerer, A. Endosomal trafficking in metabolic homeostasis and diseases. *Nat Rev Endocrinol* **19**, 28-45, doi:10.1038/s41574-022-00737-9 (2023).
32. Kjolby, M. *et al.* Sort1, Encoded by the Cardiovascular Risk Locus 1p13.3, Is a Regulator of Hepatic Lipoprotein Export. *Cell Metabolism* **12**, 213-223, doi:10.1016/j.cmet.2010.08.006 (2010).
33. Goettsch, C., Kjolby, M. & Aikawa, E. Sortilin and Its Multiple Roles in Cardiovascular and Metabolic Diseases. *Arterioscler Thromb Vasc Biol* **38**, 19-25, doi:10.1161/ATVBAHA.117.310292 (2018).
34. Blondeau, N., Beraud-Dufour, S., Lebrun, P., Hivelin, C. & Coppola, T. Sortilin in Glucose Homeostasis: From Accessory Protein to Key Player? *Front Pharmacol* **9**, 1561, doi:10.3389/fphar.2018.01561 (2018).
35. Gustafsen, C. *et al.* The hypercholesterolemia-risk gene SORT1 facilitates PCSK9 secretion. **19**, 310-318 (2014).
36. Li, J. *et al.* Neurotensin is an anti-thermogenic peptide produced by lymphatic endothelial cells. **33**, 1449-1465. e1446 (2021).
37. Carlo, A.-S., Nykjaer, A. & Willnow, T. E. J. J. o. m. m. Sorting receptor sortilin—a culprit in cardiovascular and neurological diseases. **92**, 905-911 (2014).
38. Willnow, T. E., Petersen, C. M. & Nykjaer, A. J. N. R. N. VPS10P-domain receptors—regulators of neuronal viability and function. **9**, 899-909 (2008).
39. Petersen, C. M. *et al.* Propeptide cleavage conditions sortilin/neurotensin receptor-3 for ligand binding. **18**, 595-604 (1999).
40. Ouyang, S., Jia, B., Xie, W., Yang, J. & Lv, Y. J. J. o. c. p. Mechanism underlying the regulation of sortilin expression and its trafficking function. **235**, 8958-8971 (2020).
41. Teslovich, T. M. *et al.* Biological, clinical and population relevance of 95 loci for blood lipids. **466**, 707-713 (2010).
42. Samani, N. J. *et al.* Genomewide association analysis of coronary artery disease. **357**, 443-453 (2007).
43. Lidell, M. E. *et al.* Evidence for two types of brown adipose tissue in humans. *Nat Med* **19**, 631-634, doi:10.1038/nm.3017 (2013).
44. Shinoda, K. *et al.* Genetic and functional characterization of clonally derived adult human brown adipocytes. *Nat Med* **21**, 389-394, doi:10.1038/nm.3819 (2015).
45. Schrøder, T. J. *et al.* The identification of AF38469: an orally bioavailable inhibitor of the VPS10P family sorting receptor Sortilin. **24**, 177-180 (2014).
46. Rosina, M. *et al.* Ejection of damaged mitochondria and their removal by macrophages ensure efficient thermogenesis in brown adipose tissue. *Cell Metab* **34**, 533-548 e512, doi:10.1016/j.cmet.2022.02.016 (2022).
47. Srivastava, G. & Apovian, C. M. J. N. R. E. Current pharmacotherapy for obesity. **14**, 12-24 (2018).
48. Vitali, A. *et al.* The adipose organ of obesity-prone C57BL/6J mice is composed of mixed white and brown adipocytes. **53**, 619-629 (2012).

49. Vasconcelos, J., Freire, E., Almendra, R., Silva, G. L. & Santana, P. J. E. p. The impact of winter cold weather on acute myocardial infarctions in Portugal. **183**, 14-18 (2013).
50. Bhadada, S. V., Patel, B. M., Mehta, A. A., Goyal, R. K. J. T. A. i. E. & Metabolism. β 3 receptors: Role in cardiometabolic disorders. **2**, 65-79 (2011).
51. Li, L. O. *et al.* Liver-specific loss of long chain acyl-CoA synthetase-1 decreases triacylglycerol synthesis and β -oxidation and alters phospholipid fatty acid composition. **284**, 27816-27826 (2009).
52. Coleman, R. A. J. J. o. l. r. It takes a village: channeling fatty acid metabolism and triacylglycerol formation via protein interactomes. **60**, 490-497 (2019).
53. Li, L. O. *et al.* Compartmentalized acyl-CoA metabolism in skeletal muscle regulates systemic glucose homeostasis. **64**, 23-35 (2015).
54. Al-Akhrass, H. *et al.* Sortilin limits EGFR signaling by promoting its internalization in lung cancer. **8**, 1-15 (2017).
55. Tsuchiya, Y. *et al.* Palmitate-induced down-regulation of sortilin and impaired GLUT4 trafficking in C2C12 myotubes. **285**, 34371-34381 (2010).
56. Lui, A., Sparks, R., Patel, R. & Patel, N. A. J. I. J. o. M. S. Identification of Sortilin Alternatively Spliced Variants in Mouse 3T3L1 Adipocytes. **22**, 983 (2021).
57. Olsen, J. M. *et al.* Glucose uptake in brown fat cells is dependent on mTOR complex 2-promoted GLUT1 translocation. *J Cell Biol* **207**, 365-374, doi:10.1083/jcb.201403080 (2014).
58. Aslund, A. *et al.* Myosin 1c: A novel regulator of glucose uptake in brown adipocytes. *Mol Metab* **53**, 101247, doi:10.1016/j.molmet.2021.101247 (2021).
59. Olsen, J. M. *et al.* Glucose uptake in brown fat cells is dependent on mTOR complex 2-promoted GLUT1 translocation. **207**, 365-374 (2014).
60. Rudich, A. *et al.* Indinavir uncovers different contributions of GLUT4 and GLUT1 towards glucose uptake in muscle and fat cells and tissues. *Diabetologia* **46**, 649-658, doi:10.1007/s00125-003-1080-1 (2003).
61. Cullen, P. J. & Steinberg, F. To degrade or not to degrade: mechanisms and significance of endocytic recycling. *Nat Rev Mol Cell Biol* **19**, 679-696, doi:10.1038/s41580-018-0053-7 (2018).
62. Krahmer, N. *et al.* Organellar Proteomics and Phospho-Proteomics Reveal Subcellular Reorganization in Diet-Induced Hepatic Steatosis. *Dev Cell* **47**, 205-221 e207, doi:10.1016/j.devcel.2018.09.017 (2018).
63. Xue, B. *et al.* Effects of High Fat Feeding on Adipose Tissue Gene Expression in Diabetic Goto-Kakizaki Rats. *Gene Regul Syst Bio* **9**, 15-26, doi:10.4137/GRSB.S25172 (2015).

Figures

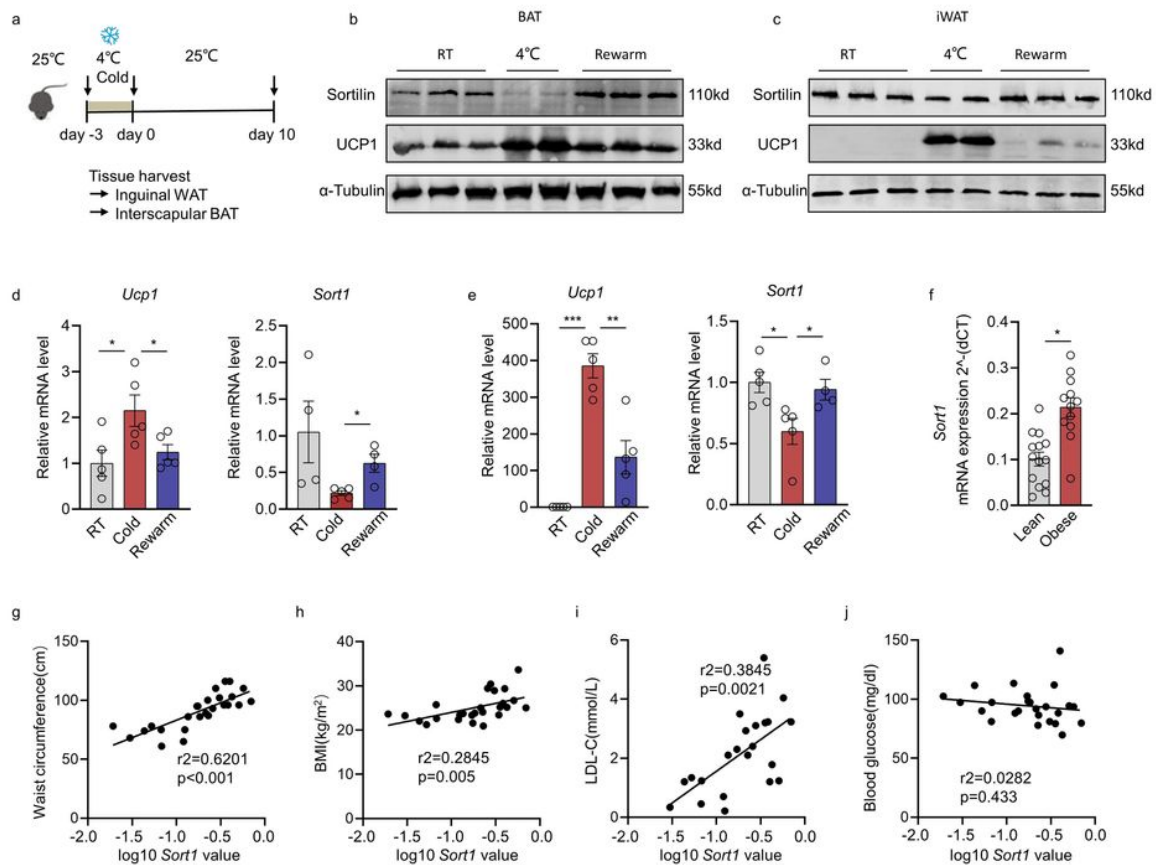


Figure 1

Sortilin expression is reduced upon cold stimulation and is positively associated with obesity

(a) Workflow of cold challenge and rewarm for WT mice;

(b-c) Immunoblot analysis of sortilin and UCP1 in BAT(b) and iWAT(c) after cold challenge and rewarm;

(d-e) mRNA analysis of *Sort1* and *Ucp1* in BAT(d) and iWAT(e) after cold challenge and rewarm.

(f) Detection of the mRNA expression of *Sort1* in omental adipose tissues from obese and lean patients.

(g-j) Analysis of the correlation between *Sort1* expression and waist circumference(g), BMI(h), LDL-C(i) and blood glucose(j).

Statistical significance was assessed by two-tailed Student's t test. Values were presented as Pearson's r correlation coefficient(g-j). Data are presented as mean \pm SEMs and * $p < 0.05$, ** $p < 0.01$, *** $p < 0.001$.

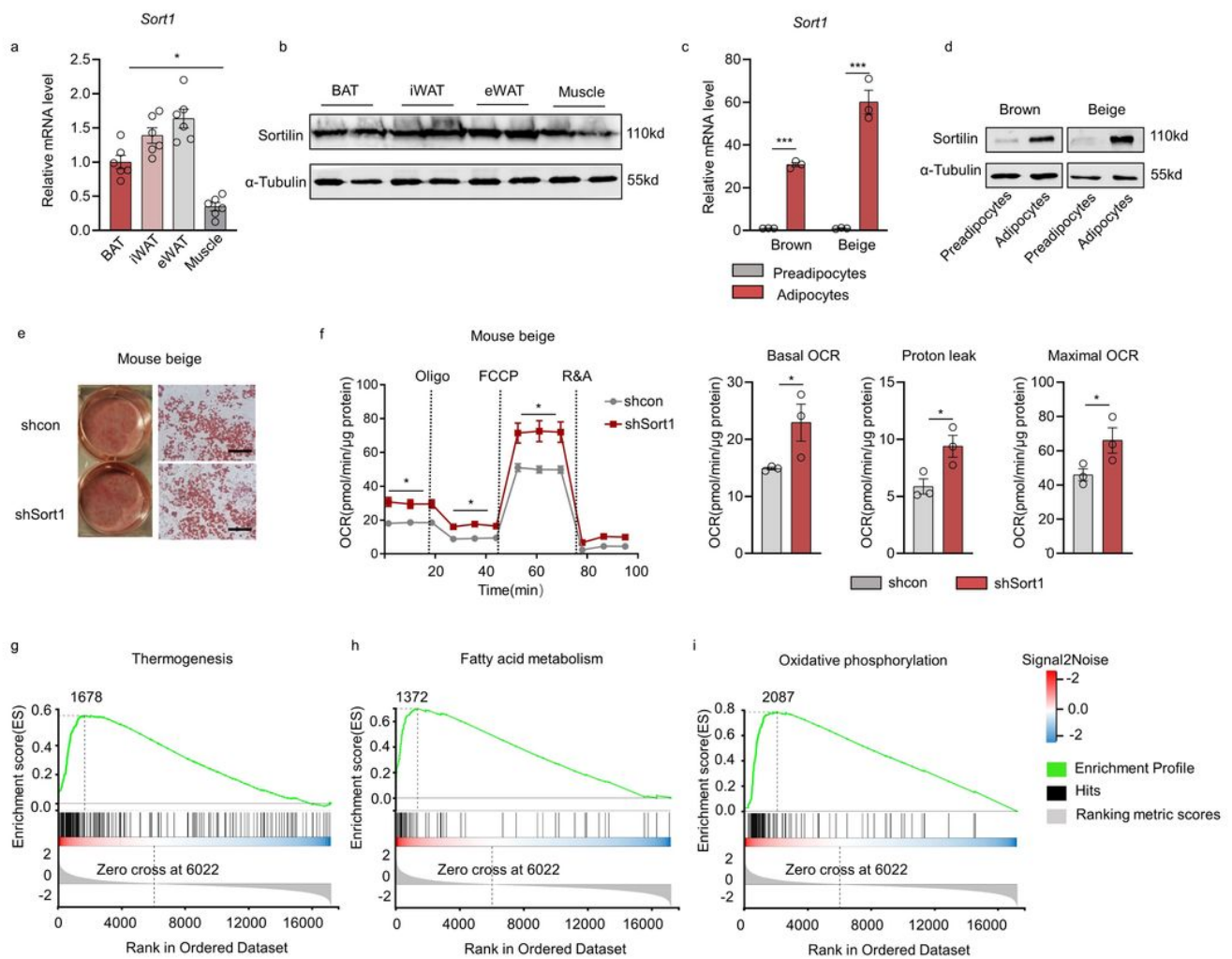


Figure 2

***Sort1* depletion enhances fat thermogenesis**

(a) The mRNA expression levels of *Sort1* were evaluated in mouse adipose tissues (epididymal, inguinal and brown) and muscle.

(b) Immunoblot analysis of sortilin in mouse adipose tissues (epididymal, inguinal and brown) and muscle.

(c) The mRNA expression levels of *Sort1* were evaluated in preadipocytes and differentiated brown and inguinal adipocytes.

(d) Immunoblot analysis of sortilin in preadipocytes and differentiated brown and inguinal adipocytes.

(e) Oil Red O staining of fully differentiated beige adipocytes expressing shRNA targeting *Sort1*(shSort1) as compared a scrambled control (shcon). Scale bar: 50 μ m.

(f) OCR was monitored by Seahorse analyzer in shcon and shSort1 mouse beige adipocytes.

(g-i) GSEA analysis of thermogenesis(g), fatty acid metabolism(h) and oxidative phosphorylation(i) pathway in shSort1 beige adipocyte compared with shcon.

Statistical significance was assessed by two-tailed Student's t test or two-way ANOVA (a). Data are presented as mean \pm SEMs and *p < 0.05, ***p < 0.001.

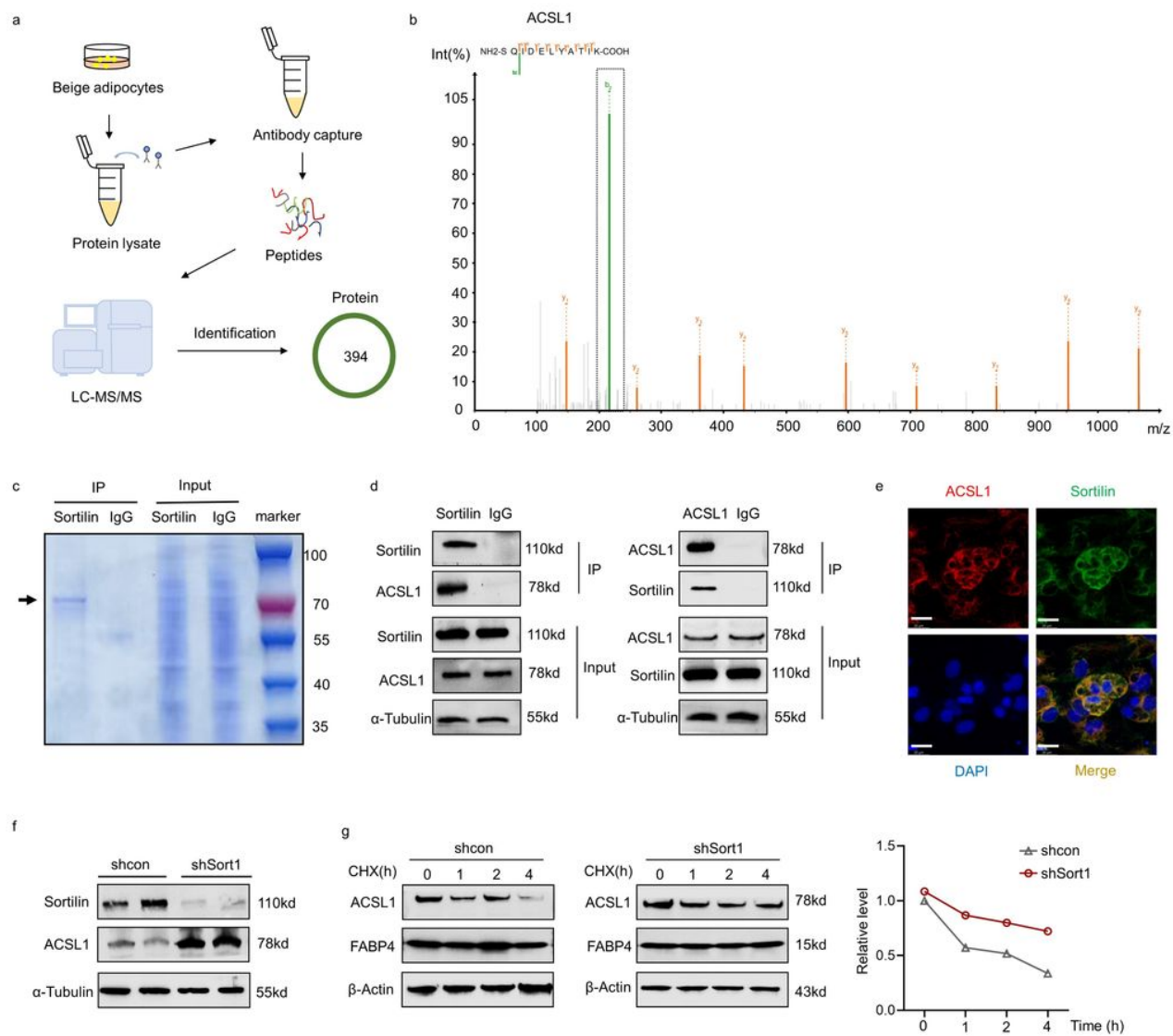


Figure 3

Sortilin interacts with ACSL1 and controls its protein degradation

(a) Workflow of IP by sortilin and vehicle IgG antibody for protein capture by mass spectrometry-based proteomics.

(b) Identification of ACSL1 as an interactor of sortilin by LC-MS/MS in beige adipocytes.

(c) IP assay using sortilin antibody or IgG. Samples were run on Bis-Tris Gel and then stained with Coomassie Blue Staining.

(d) Co-IP assay showing interaction between sortilin and ACSL1 using sortilin antibody (left) or ACSL1 antibody (right).

(e) Representative images of immunofluorescence for sortilin (green), ACSL1 (red), and nuclei (blue) in beige adipocytes. Scale bar: 20 μm .

(f) Immunoblot analysis of ACSL1 in shcon and shSort1 beige adipocytes.

(g) Cycloheximide (CHX)-chase assay showing the degradation of ACSL1 in shcon and shSort1 beige adipocytes. The quantification is shown at right.

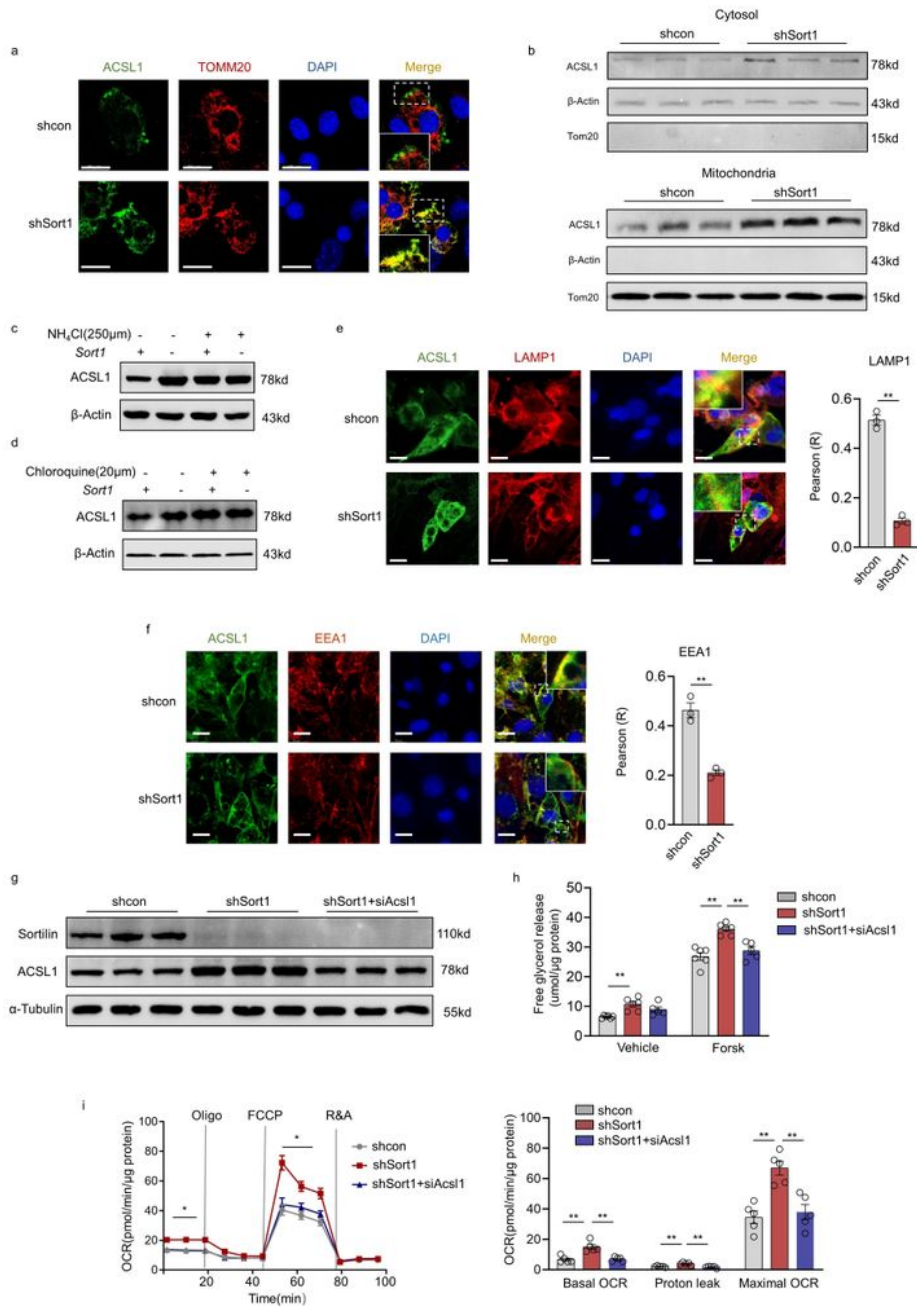


Figure 4

Sortilin targets mitochondrial ACSL1 to lysosomal degradation to regulate thermogenesis

(a) Representative images of immunofluorescence for ACSL1 (green), TOMM20 (red), and nuclei (blue) in shcon and shSort1 beige adipocytes. Scale bar: 20 μm.

(b) Immunoblot analysis of ACSL1 on mitochondria and cytosol of shcon and shSort1 beige adipocytes. β -actin and TOMM20 band were used for loading control.

(c-d) Immunoblots showing the effect of sortilin on ACSL1 expression in the absence and presence of lysosomal inhibitors NH₄Cl and chloroquine. This experiment was repeated three times independently with similar results.

(e-f) Immunofluorescence showing the colocalization between ACSL1 and LAMP1 (e) or EEA1 (f) in shcon and shSort1 beige adipocytes. Scale bars indicate 20 μ m. The statistical results of colocalization factor (Pearson's R value) were shown on the right panel.

(g) Immunoblot analysis of ACSL1 in shcon, shSort1 and shSort1+siACSL1 beige adipocytes.

(h) Glycerol accumulation during 12h in supernatant of shcon, shSort1 and shSort1+siACSL1 beige adipocytes.

(i) OCR measurement in shcon, shSort1 and shSort1+siACSL1 beige adipocytes.

Statistical differences were determined by two-tailed Student's t-test; Data are presented as mean \pm SEMs and *p < 0.05, **p < 0.01 compared to control group.

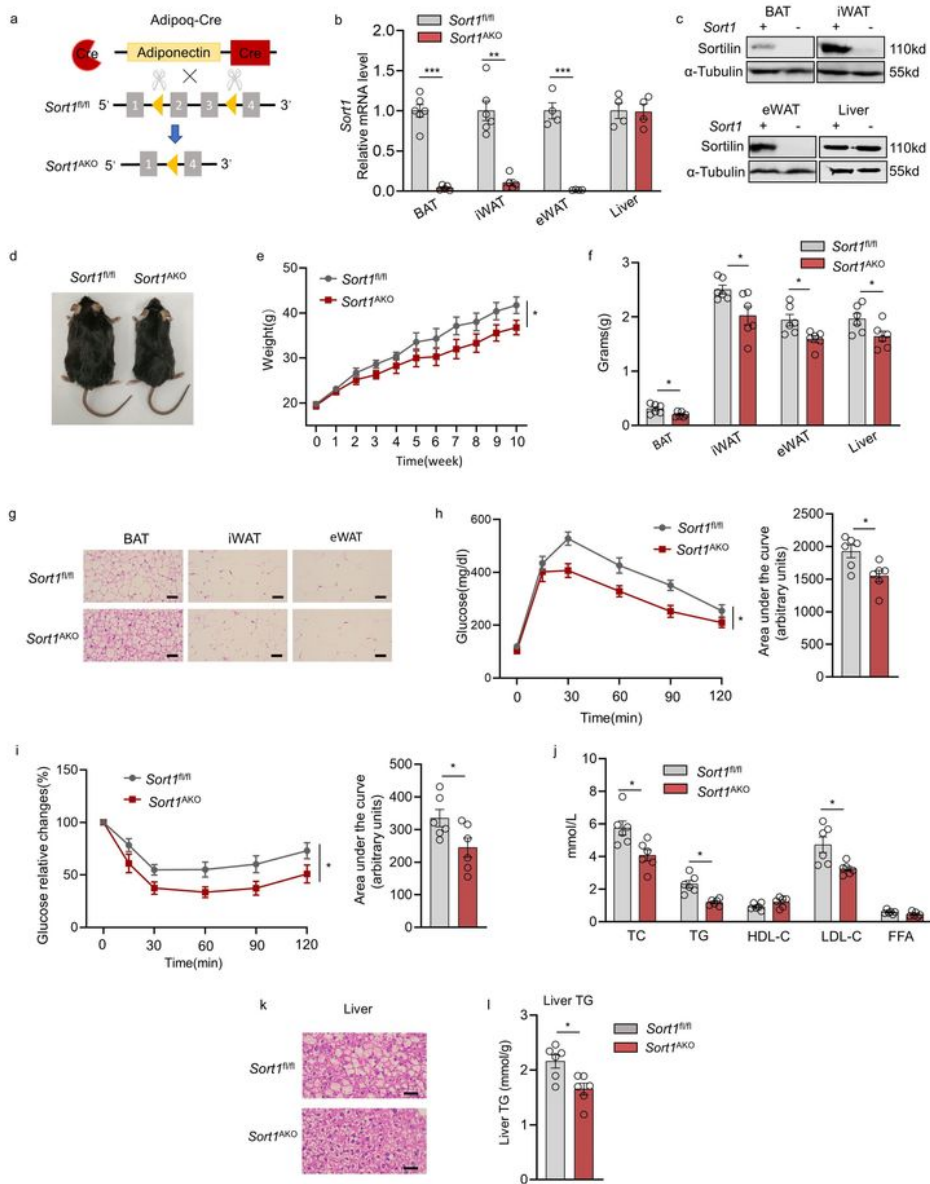


Figure 5

Fat-specific loss of *Sort1* restrains the development of HFD-induced obesity

(a) Overview of *Sort1*^{AKO} mice model.

(b) The mRNA expression of *Sort1* in iWAT, eWAT, BAT and liver.

- (c) Immunoblot analysis of sortilin in iWAT, eWAT, BAT and liver.
- (d) Representative photo of HFD induced obesity in *Sort1*^{AKO} and *Sort1*^{fl/fl} mice.
- (e) Body weight of HFD induced obesity in *Sort1*^{AKO} and *Sort1*^{fl/fl} mice.
- (f) Weights of fat tissues and liver in *Sort1*^{AKO} and *Sort1*^{fl/fl} mice.
- (g) Representative H&E staining images of dissected tissues in *Sort1*^{AKO} and *Sort1*^{fl/fl} mice. Scale bar: 20µm.
- (h-i) Intraperitoneal glucose tolerance test (GTT) (h) and insulin tolerance test (ITT) (i) in *Sort1*^{AKO} and *Sort1*^{fl/fl} mice.
- (j) Serum lipid profile of *Sort1*^{AKO} and *Sort1*^{fl/fl} mice.
- (k) Representative HE-staining images of liver from *Sort1*^{AKO} and *Sort1*^{fl/fl} mice under HFD. Scalebar: 20µm.
- (l) Triglyceride content in liver tissues of *Sort1*^{AKO} and *Sort1*^{fl/fl} mice.

Statistical significance was assessed by two-tailed Student's t test or ANCOVA (e, h and i). Data are presented as mean ± SEMs. Significance was assessed by *p < 0.05, **p < 0.01, ***p < 0.001 compared to control group.

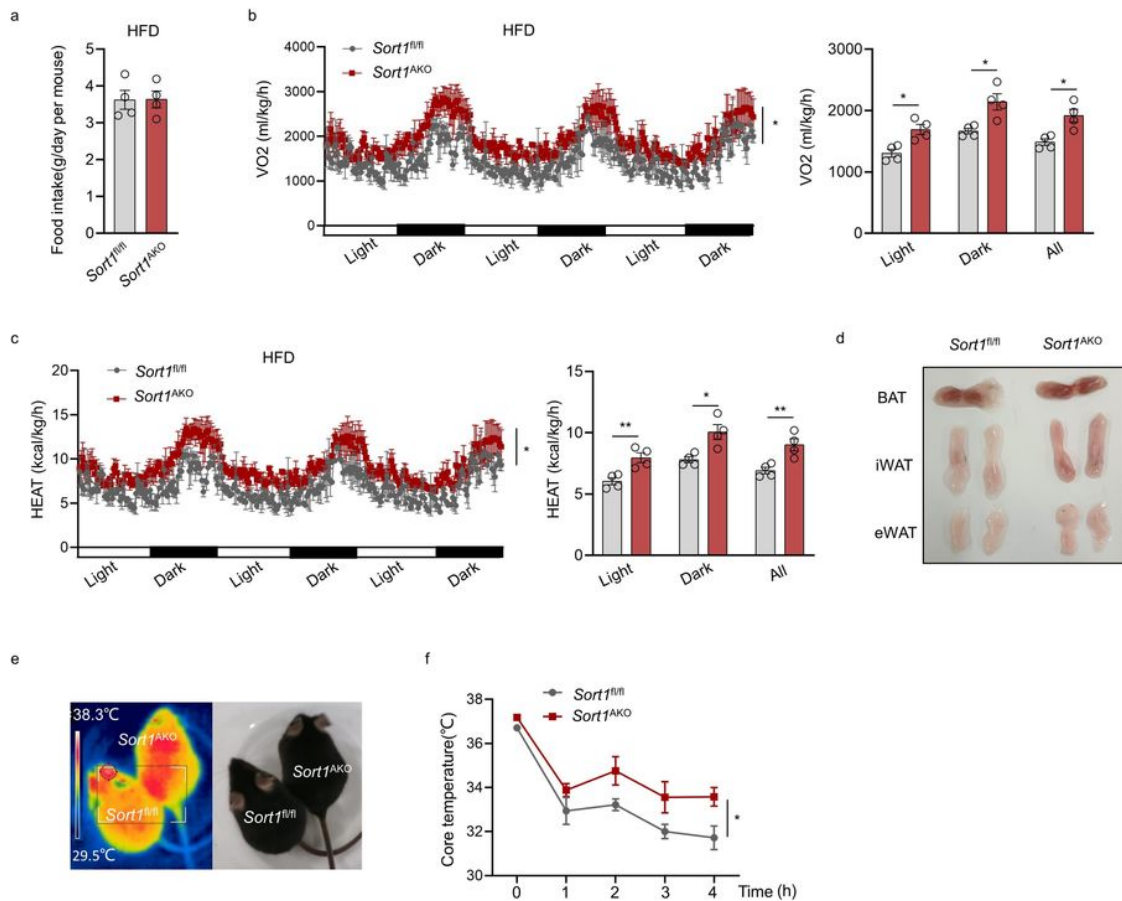


Figure 6

Fat-specific loss of *Sort1* promotes thermogenesis and energy expenditure

(a) Food intake of *Sort1*^{AKO} and *Sort1*^{fl/fl} mice fed HFD.

(b-c) Whole-body oxygen consumption (VO₂) and energy expenditure (HEAT) normalized by body weight under basal conditions (22°C) in *Sort1*^{AKO} and *Sort1*^{fl/fl} mice fed HFD.

(d) Representative photo of fat pads of *Sort1*^{AKO} and *Sort1*^{fl/fl} mice under chow diet.

(e) Representative thermal images as shown by FLIR image in *Sort1*^{AKO} and *Sort1*^{fl/fl} mice.

(f) The rectal temperature of *Sort1*^{AKO} and *Sort1*^{fl/fl} mice fed HFD in response to a cold challenge(4 °C) from TN(30 °C) for at least 7 days.

Statistical significance was assessed by two-tailed Student's t test or ANCOVA (b-c and f). Data are presented as mean ± SEMs. Significance was assessed by *p < 0.05, **p < 0.01 compared to control group.

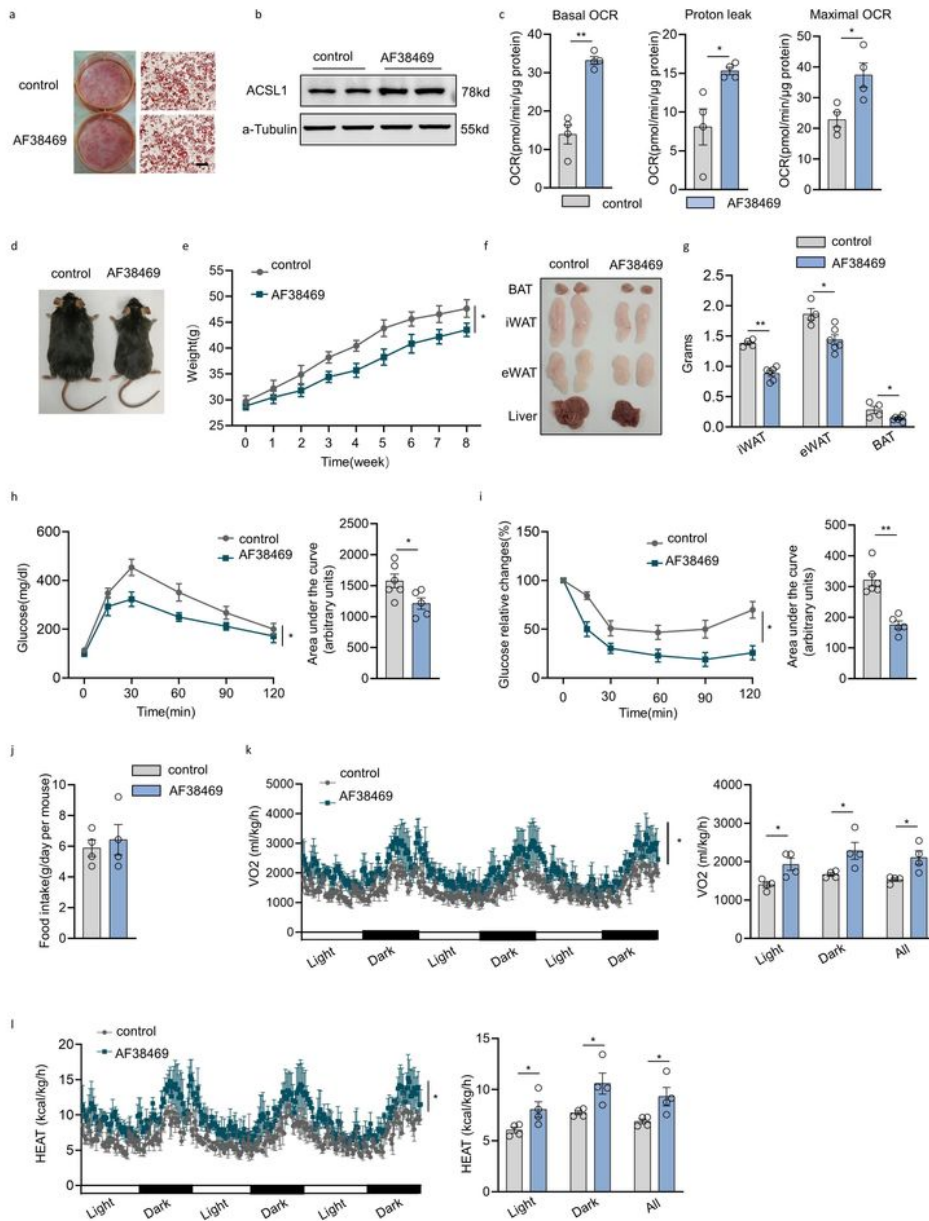


Figure 7

Sortilin inhibitor AF38469 promotes fat thermogenesis with promising therapeutic potential

- (a) Oil Red O staining of beige adipocytes treated with AF38469 compared with vehicle. Scale bar: 50 μ m.
- (b) Immunoblot analysis of ACSL1 were evaluated in beige adipocytes treated with AF38469 or vehicle.
- (c) OCR was monitored by Seahorse analyzer in AF38469 or vehicle treated beige adipocytes.
- (d-i) Analysis of metabolic performances of mice chronically treated with AF38469 dissolved in water compared with vehicle, as described in (d) representative photo of mice, (e) body weight, (f) representative photos of fat pad morphology and liver, (g) fat weight, (h) GTT and (i) insulin tolerance test (ITT).
- (j) Food intake of AF38469 and vehicle treated mice.
- (k-l) Whole-body oxygen consumption(k) and energy expenditure (l) of AF38469 and vehicle treated mice.

Statistical significance was assessed by two-tailed Student's t test or ANCOVA (e, h, i, k and l). Data are presented as mean \pm SEMs. Significance was assessed by * $p < 0.05$, ** $p < 0.01$ compared to control group.

Supplementary Files

This is a list of supplementary files associated with this preprint. Click to download.

- [SupplTable.docx](#)
- [Supplementalinformation.docx](#)
- [abstractgraphic.jpg](#)
- [ExtendedDataFig1.jpg](#)
- [ExtendedDataFig2.jpg](#)
- [ExtendedDataFig3.jpg](#)
- [ExtendedDataFig4.jpg](#)
- [ExtendedDataFig51.jpg](#)
- [ExtendedDataFig52.jpg](#)
- [ExtendedDataFig6.jpg](#)